Protein Engineering, Design and Selection, 2019, vol. 32 no. 6, pp. 277–288
doi: 10.1093/protein/gzz046
Advance Access Publication Date: 23 December 2019
Original Article

OXFORD

Original Article

Electrostatic interactions modulate the differential aggregation propensities of IgG1 and IgG4P antibodies and inform charged residue substitutions for improved developability

James T. Heads*, Richard Lamb, Sebastian Kelm, Ralph Adams, Peter Elliott, Kerry Tyson, Sarfaraj Topia, Shauna West, Ruodan Nan, Alison Turner, and Alastair D. G. Lawson

UCB Pharma, Slough, Berkshire SL1 3WE, UK

*To whom correspondence should be addressed. E-mail: james.heads@UCB.com

Paper Edited by: Daniel Christ, PEDS Board Member

Received 22 July 2019; Revised 17 October 2019; Editorial Decision 5 November 2019; Accepted 19 November 2019

Abstract

Native state aggregation is an important concern in the development of therapeutic antibodies. Enhanced knowledge of mAb native state aggregation mechanisms would permit sequence-based selection and design of therapeutic mAbs with improved developability. We investigated how electrostatic interactions affect the native state aggregation of seven human IgG1 and IgG4P mAb isotype pairs, each pair having identical variable domains that are different for each set of IgG1 and IgG4P constructs. Relative aggregation propensities were determined at pH 7.4, representing physiological conditions, and pH 5.0, representing commonly used storage conditions. Our work indicates that the net charge state of variable domains relative to the net charge state of the constant domains is predominantly responsible for the different native state aggregation behavior of IgG1 and IgG4P mAbs. This observation suggests that the global net charge of a multi domain protein is not a reliable predictor of aggregation propensity. Furthermore, we demonstrate a design strategy in the frameworks of variable domains to reduce the native state aggregation propensity of mAbs identified as being aggregation-prone. Importantly, substitution of specifically identified residues with alternative, human germline residues, to optimize Fv charge, resulted in decreased aggregation potential at pH 5.0 and 7.4, thus increasing developability.

Key words: aggregation, antibody, Fab, Fv, IgG1, IgG4P, isotype, mAb, prediction

Introduction

The increasingly high cost of developing potential therapeutic antibodies necessitates that development time and attrition rates are as low possible (Kola and Landis, 2004). Developing methodologies that enable selection of molecules with beneficial biophysical properties, thereby increasing the probability of selecting a successful lead candidate, is vital (Jarasch *et al*., 2015). Many of the diseases that are targeted by mAbs are chronic and require frequent dosing from high stock concentrations (>100 mg/mL) (Shire *et al*., 2004). The manufacture of such products is challenging, in large part due to the potential for aggregation. Protein–protein interactions become more frequent as product concentration is increased and can, under certain conditions, result in a greater probability of aggregate formation (Laue, 2012). This is a fundamental concern because aggregates can elicit adverse immune reactions, alter the pharmacokinetic profile and compromise clinical efficacy (Baert *et al*., 2003; Moussa *et al*., 2016; Pineda *et al*., 2016; Singh, 2011). It is therefore highly desirable that lead candidates have low aggregation propensity.

All currently approved therapeutic mAbs belong to the IgG class, which is divided up into several isotypes. Selection of isotype is typically based on the required interaction with the human immune system. Briefly, the IgG1 subclass can be used when the required mechanism of action relies on antibody-dependent cellular cytotoxicity (ADCC) and complement-dependent cytotoxicity (CDC). IgG4 antibodies demonstrate significantly weaker ADCC and CDC activity (Vidarsson *et al*., 2014) and are therefore often the therapeutic format of choice when effector function engagement is not required.

While the IgG1 and IgG4 subclasses show high sequence homology, small but significant differences are evident at specific positions in their sequences, hinge lengths and inter-chain disulfide bond (DSB) arrangements. They are hetero-tetramers of approximately 150 kDa, which are composed of two pairs of heavy and light chain polypeptides linked by DSBs. The heavy chain contains a variable (V_H) domain and three constant domains, C_{H1}, C_{H2} and C_{H3}. The light chain can be one of two types, Lambda or Kappa, and contains a variable (V_L) and a single constant (C_L) domain. In contrast to the constant domains, the variable domains exhibit extensive sequence diversity that enables antigen recognition. This domain is subdivided into framework regions and complementarity determining regions (CDR); the framework acts a scaffold for the CDRs. An undesirable side effect of variable region sequence diversity is the broad range of aggregation propensities observed for mAbs (Jain *et al*., 2017). Antigen affinity is determined by several factors, including electrostatic interactions, hydrogen bonds, Van der Waals contacts and hydrophobicity. Unsurprisingly, these interactions allow antibody molecules in their native folded state to attract each other leading to the potential for aggregation events.

Understanding the pH-dependent aggregation propensity of mAbs would be advantageous for efficient drug development. Typical pH values encountered by mAbs *in vivo* range from neutral to slightly acidic (Roopenian and Akilesh, 2007). During manufacture, storage and administration mAbs are exposed to a range of acidic and basic conditions (Liu *et al*., 2010; Shire, 2009; Wang *et al*., 2007). The buffer systems required by these processes can dramatically alter the molecules' charge states, which may elicit unfavourable electrostatic interactions resulting in the formation of aggregates, thus affecting yield (Cromwell *et al*., 2006). Prior knowledge of pH-dependent native state aggregation propensity would therefore be beneficial. Additionally, improved knowledge of mAb aggregation mechanisms would enable rationally designed residue substitutions that reduce aggregation propensity.

We undertook a detailed analysis of human IgG1 and human IgG4P mAb native state aggregation at neutral and slightly acidic pH, both of which are commonly encountered during manufacture and *in vivo*. We examined how the complex interactions of electrostatic forces affected the native state aggregation propensity of seven unrelated Fv domains formatted as human IgG1 and IgG4P mAbs. Using experimentally derived data, we generated a mAb native state aggregation prediction model based on simple sequence charge descriptors. This model system enabled the design of specific residue substitutions that decreased native state aggregation, thereby improving candidate developability.

Materials and Methods

Antibody gene generation

Seven unique Fv domains were formatted as human IgG1 and IgG4P mAbs. The IgG4P mAbs contained a S241P mutation in the hinge region to reduce the formation of half antibody associated with the IgG4 isotype (Angal *et al*., 1993). All samples contain Kappa light chains. Residue substitutions were introduced by site-directed mutagenesis. Oligonucleotides were designed to substitute the desired residues (Sigma, UK). PCR reactions were set up to substitute bases using QuikChange Lightning Multi Site-Directed Mutagenesis Kit (Agilent, 210514). DNA constructs were verified by Sanger sequencing.

Transient expression of samples

Samples were transiently expressed in Expi293F^{TM} cells (Thermofisher Scientific, A14528). Prior to transfection, the cells were centrifuged for eight minutes and suspended in fresh Expi293^{TM} Expression Medium (Thermofisher Scientific, A1435103) at a density of 3×10^6 cells/mL with cell viabilities of 95% and above achieved. Plasmids encoding for the light and heavy chains of the antibodies (100 µg total) were transfected into the cells by preparing an Expifectamine/OptiMEM^{TM} (Thermofisher Scientific, A1435103) solution. Cells were grown for 18–20 h at 37°C, 125 rpm and 8% CO_2 atmosphere in 1-l plastic Erlenmeyer flasks with ventilated caps (Corning®, 431403) in a shaking incubator. After this time ExpiFectamine^{TM} 293 Transfection Enhancers 1 and 2 (Thermofisher Scientific, A14524) were added to the cells. Using the conditions previously stated, cells were grown for a further seven days. Samples were harvested by centrifugation for 30 min; the cells were discarded and the supernatant was filtered through a 0.22-µm filter.

Purification of samples

Samples were purified using a two-step purification process. A 5-mL HiTrap MabSelect SuRe column, (GE healthcare, 11003494) and a HiLoad 16/600 and Superdex 200 prep grade gel filtration column (GE healthcare, 28989335) were attached to an ÄKTAXpress (GE healthcare, 18664501). The MabSelect Sure column was equilibrated in PBS pH 7.4 and the supernatant was applied at a flow rate of 5 mL/min. The column was washed with PBS pH 7.4 and the bound material was eluted with 0.1 M of sodium citrate, pH 3.6 and neutralized with a one-fifth volume of 2 M tris-HCl pH 8.5. The eluted material was then applied to an S200 16/60 column equilibrated into PBS, at a flow rate of 1 mL/min. The final purity, threshold set at > 95%, was determined by size exclusion chromatography (SEC) on an analytical TSKgel G3000SW$_{XL}$ (MERCK, 808541), developed with an isocratic gradient of PBS at 1.0 mL/min.

Sample preparation

Samples were filtered through a 0.22-µm filter and buffer exchanged into PBS pH 7.4 or 50 mM of sodium acetate 125 mM of sodium chloride pH 5.0 using Slide-A-Lyzer^{TM} MINI dialysis device 10 K MWCO (ThermoFisher Scientific, 88401), following the manufacturer's instructions. For clarity, these buffers will be referred to by their pH value in the result and discussion sections of the manuscript.

Polyethylene glycol (PEG) aggregation assay

Stock PEG 3350 (Merck, 202444) solutions (w/v) were prepared in PBS pH 7.4 or 50 mM sodium acetate. 125 mM sodium chloride pH 5.0. A 1:1.1 serial titration was performed by an assist plus liquid handling robot (Integra, 4505) to avoid liquid handling issues; the stock concentration of PEG 3350 was capped at 40%. To minimize nonequilibrium precipitation, sample preparation consisted of mix-

ing protein and PEG solutions at a 1:1 volume ratio. 35 µL of the PEG 3350 stock solution was added to a 96 well V bottom PCR plate (A1 to H1) by a liquid handling robot. 35 µL of a 2 mg/mL of sample solution (unless otherwise stated) was added to the PEG stock solutions resulting in a 1 mg/mL of test concentration. This solution was mixed by automated slow repeat pipetting and incubated at 37°C for 0.5 h to re-dissolve any nonequilibrium aggregates. Samples were then incubated at 20°C for 24 h. The sample plate was subsequently centrifuged at 4000 × g for 1 h at 20°C. 50 µL of supernatant was dispensed into a UV-Star®, half area, 96 well, µClear®, microplate (Greiner, 675801). Protein concentrations were determined by UV spectrophotometry at 280 nm using a FLUOstar Omega multi-detection microplate reader (BMG LABTECH). The resulting values were plotted using Graphpad prism ver 7.04; PEG midpoint (PEG_{mdpnt}) score was derived from the midpoint of the sigmoidal dose-response (variable slope) fit.

Method for the determination of calculated pI and charge

The isoelectric point (pI) was calculated from an amino acid sequence using the following method. A molecular charge vs. pH plot was generated by iterating over a range of pH values (from 1.0 to 14.0, in increments of 0.1). At each pH, every titratable residue's partial charge, C_p, was calculated using the formulas.

$C_p = 1/(10^{(pH-pKa)} + 1)$ for His, Arg, Lys and the N-terminus
$C_p = 1/(10^{(pH-pKa)} + 1) - 1$ for Asp, Glu, Cys, Tyr and the C-terminus.

The C_p values were summed over the entire sequence to calculate the molecular charge. Cysteines were assumed to form disulfide bonds and were not included in the calculation unless an odd number of cysteines were present. In the latter case, a single cysteine was included. The pI was determined to be the pH value at which the molecular charge was closest to zero (Lehninger *et al*., 2008).

Fluorescence-based thermal stability (T_m) measurement

A thermal stability assay was performed to assess conformational stabilities of purified molecules. The reaction mix contained 5 µL of 30× SYPRO™ Orange Protein Gel Stain (Thermofisher scientific, S6651), diluted from 5000× concentrate with test buffer. 45 µL of sample at 0.2 mg/mL, in PBS pH 7.4, or 50 mM sodium acetate 125 mM sodium chloride pH 5.0, was added to the dye and mixed, 10 µL of this solution was dispensed in quadruplicate into a 384 PCR optical well plate and was run on a QuantStudio 7 Real-Time PCR System (Thermofisher). The PCR system heating device was set at 20°C and increased to 99°C at a rate of 1.1°C/min. A charge-coupled device monitored fluorescence changes in the wells. Fluorescence intensity increases were plotted and the inflection point of the slope(s) was used to generate apparent midpoint temperatures (T_m). Domain assignments were made by reference to the known T_ms of the C_{H2} and C_{H3} domains in each test buffer.

Hydrophobic interaction chromatography (HIC)

A Dionex ProPac HIC − 10 column of 100 × 4.6 mm (ThermoFisher scientific, 063655) was used to rank apparent hydrophobicity. All separations were carried out on an Agilent HP1260 HPLC (Agilent) equipped with a fluorescence detector. The column temperature was maintained at 20°C throughout the run and flow rate was set at 0.8 mL/min. The mobile phase for the HIC method consisted of 0.8 M ammonium sulfate, 50 mM phosphate pH 7.4 or 0.8 M ammonium sulfate, 50 mM sodium acetate pH 5.0 (buffer A) and 50 mM phosphate pH 7.4 or 50 mM sodium acetate pH 5.0 (buffer B). Following a 5 min hold at 0% B, bound protein was eluted using a linear gradient from 0 to 100% B over 45 min and the column was washed with 100% B for 2 min and re-equilibrated in 0% B for 10 min. The separation was monitored by intrinsic fluorescence with excitation occurring at 280 nm and emission at 340 nm.

Biacore affinity assay

For $mAbX_{IgG4P}$, the assay format was capture of mAb by immobilized anti-human IgG Fc followed by titration of ligand over the captured surface. Biomolecular interaction analysis using surface plasmon resonance technology (SPR) was performed on a Biacore T200 system (GE Healthcare Bio-Sciences AB). Affinipure $F(ab')_2$ fragment goat anti-human IgG, Fc fragment specific (Jackson ImmunoResearch Lab, Inc. 109-006-098) in 10 mM of sodium acetate, pH 5.0 buffer was immobilized on a CM5 Sensor Chip (GE Healthcare, BR100012) via amine coupling chemistry to a level of approximately 5000 response units (RU) using HBS-EP+, 10 mM HEPES pH 7.4, 150 mM NaCl, 3 mM EDTA, 0.05% (v/v) Surfactant P20 as the running buffer. Samples were diluted to between 0.6 and 0.8 µg/mL in running buffer. A 60-s injection of mAb at 10 µL/min was used for capture by the immobilized anti-human IgG Fc to give a capture level of approximately 150 RU. Ligand was titrated from 40 to 0.62 µM over the captured mAb for 60 s at 30 µL/min followed by 60-s dissociation. The surface was regenerated by injections of 40 mM HCl for 60 s, 5 mM NaOH for 30 s and 40 mM HCl for 30 s at 10 µL/min. The data were analyzed using Biacore T200 evaluation software (version 3.0). Steady state fitting was used to determine affinity values.

For $mAbY_{IgG4P}$, the assay format was titration of $mAbY_{IgG4P}$ over the immobilized ligand. The ligand was prepared in 10 mM of NaAc, pH 3.5, and immobilized on flow cell surfaces of a CM5 Sensor Chip via amine coupling chemistry to reach an immobilization level of approximately 40 RU. The running buffer was HBS-EP+, pH 7.4 and $mAbY_{IgG4P}$ was injected at seven concentrations from 0.05 to 200 nM over the immobilized ligand surfaces with a contact time of 3 min and disassociation time of 30 min, at a flow rate of 100 µL/min. The surface was regenerated by two injections of 50 mM HCl, for 90 and 60 s, respectively, at a flow rate of 10 µL/min. The data were analyzed using the Biacore T200 evaluation software (version 3.0) using the bivalent analyte model with assumed no bulk contribution (RI = 0) and global Rmax.

Results

Sequence analysis of IgG1 and IgG4 mAb isotypes

To facilitate analysis of experimental data, we began our investigations by examining sequence differences between IgG subclasses. Hydrophobic residue content is similar for each counterpart constant domain of the IgG1 and IgG4P isotypes, but the number of charged residues differs between subclasses (supplementary material, **SI 1**). Electrostatic interactions are known to contribute to native state aggregation (Wang and Roberts, 2018). Thus, to compare the electrostatic potential of the two subclasses, we generated pI data for each of the constant domains by use of an in-house *in silico* pI calculator. Twelve randomly selected mAbs were measured

Table I. Summary of computationally derived pI and calculated charge at pH 7.4 and 5.0 for IgG isotypes and components thereof

Isotype	Domains	Calculated pI	Calculated charge at pH 7.4	Calculated charge at pH 5.0
IgG1	C_{H1}/C_L	9.4	3	7
	Hinge	7.8	0	1
	Fc	7.8	0	6
	C_{H2}	9.1	1	4
	C_{H3}	6.3	−1	2
IgG4P	C_{H1}/C_L	9.2	1	5
	Hinge	6.9	0	0
	Fc	6.0	−3	2
	C_{H2}	7.7	0	2
	C_{H3}	5.4	−3	0

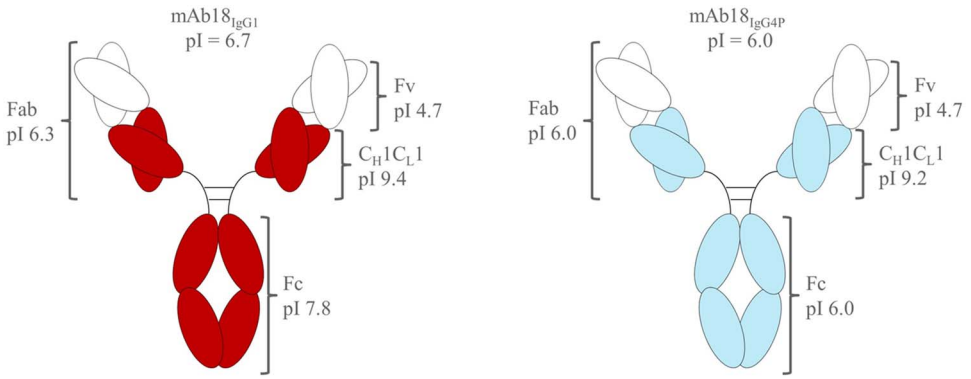

Fig. 1 Illustration showing mAb18 as an IgG1 (dark red constant domains) and IgG4P (light blue constant domains) isotypes.

experimentally by free solution cIEF to confirm that our computationally derived pI data were meaningful. An R^2 value of 0.93 was generated suggesting that calculated charge data provided a good approximation of the experimentally derived data (supplementary material, **SI 2**).

Analysis of the constant domains showed that antibody isotype had a significant impact on the pI of the molecule. Each IgG4P constant domain has an equal or greater number of acidic residues compared to the counterpart IgG1 constant domain resulting in a lower pI for IgG4P Fc domains (Table I). The C_{H1}/C_L domains and of each isotype show similarly high pI values, and the hinge regions show relatively minor differences in terms of charge. There was a substantial difference in charge for IgG1 and IgG4P Fc domains. At pH 7.4, the IgG1 Fc domain has negligible net charge, whereas the IgG4P Fc constant domain has substantial net negative charge, which is localized in the C_H3 domain. At pH 5.0, the IgG4P Fc is less positively charged than the IgG1 Fc. Therefore, an Fv domain in the context of an IgG4P mAb has a different overall net charge to the same variable region in the context of an IgG1 mAb (Fig. 1). To simplify the analysis, we compared the calculated charge of the Fv domain and the calculated charge of the Fc domain.

PEG aggregation assay

Direct measurement of native state aggregation propensity requires relatively large quantities of sample which is not usually available at the early stages of mAb discovery. To overcome this limitation, we used the PEG aggregation assay which uses relatively small amounts of protein. PEG is a nonabsorbing, nondenaturing polymer for protein; due to the inert nature of PEG, protein precipitation occurs primarily via an excluded volume effect (Atha and Ingham, 1981). It is commonly used as a fractional precipitating agent for the purification of proteins due to the reversibility of its action (Bergmann-Leitner *et al*., 2008; Knevelman *et al*., 2010; Martinez *et al*., 2019; Polson *et al*., 1964). Samples were exposed to increasing concentrations of PEG 3350; the amount of sample remaining in solution was determined by plotting absorbance at A280 nm. The determination of % PEG concentration at which half the sample had precipitated generated a PEG midpoint (PEG_{mdpnt}) score. This score permitted test molecules to be ranked on apparent native state aggregation propensity, a low PEG_{mdpnt} score ($\leq$ 10) indicates a greater propensity for native state aggregation.

In order to confirm that the PEG aggregation assay was a useful indicator of mAb native state aggregation, three samples with high PEG_{mdpnt} values ($mAb2_{IgG4P}$, $mAb3_{IgG1}$ and $mAb5_{IgG4P}$) and three samples exhibiting low PEG_{mdpnt} scores ($mAb14_{IgG4P}$, $mAb12_{IgG4P}$ and $mAb9_{IgG4P}$) were concentrated to approximately 50 mg/mL and examined for aggregation (supplementary material, **SI 3**). Upon concentration, $mAb12_{IgG4P}$ and $mAb9_{IgG4P}$ showed visible precipitation and became cloudy after 24-hour storage at 20°C. Precipitation was also observed for $mAb14_{IgG4P}$, forming an amorphous mass after 4 days. $mAb2_{IgG4P}$, $mAb3_{IgG1}$ and $mAb5_{IgG4P}$ showed no evidence of aggregation by visual inspection after two weeks of incubation at 20°C. Size exclusion high performance liquid chromatograph (SE-HPLC) data for $mAb2_{IgG4P}$, $mAb3_{IgG1}$ and $mAb5_{IgG4P}$ showed no increase in soluble aggregates over the incubation period. The area under the curves of equivalent loads for day 0 samples and day 14 samples showed no meaningful difference (supplementary material, **SI 4**).

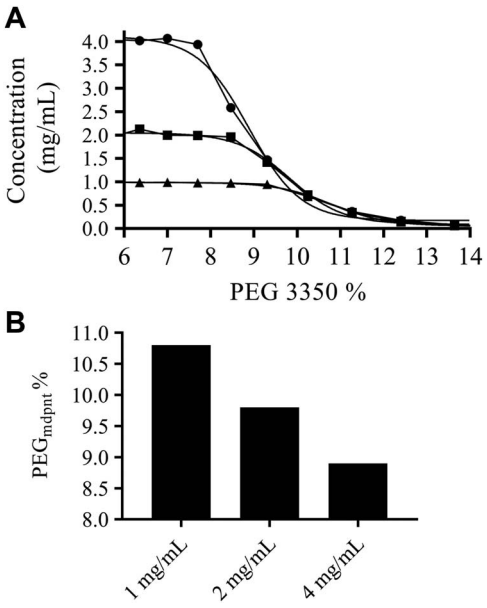

Fig. 2 (**A**) The plot shows soluble mAb concentration versus mAb PEG 3350 concentration in PBS pH 7.4 at 4 mg/mL (circles), 2 mg/mL (squares) and 1 mg/mL (triangles). A nonlinear regression sigmoidal dose response variable slope fit has been applied. (**B**) Bar chart shows PEG_{mdpnt} scores (derived from the midpoint of the slope) at the three test concentrations (insufficient sample for replicates).

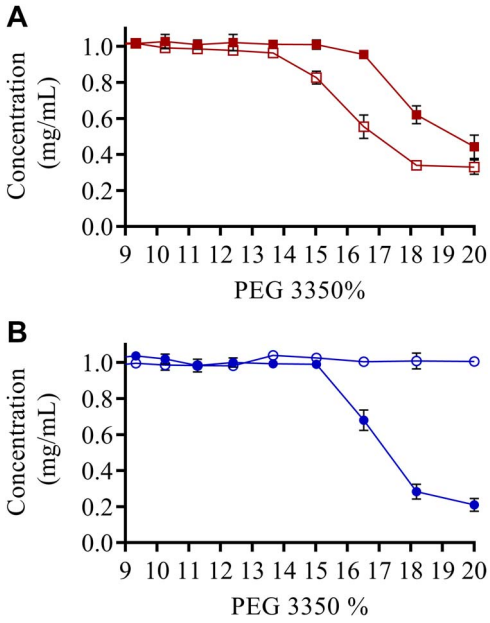

Fig. 3 The plots show soluble Fc concentration versus PEG 3350 concentration at pH 7.4 and 5.0. (**A**) Solid squares indicate IgG1 Fc pH 5.0 data points. Hollow squares indicate IgG1 Fc pH 7.4 data points. (**B**) Solid circles indicate IgG4 Fc pH 5.0 data points. Hollow circles indicate IgG4P Fc pH 7.4 data points. The error bars represent standard deviation from three independent experiments.

Further validation of the assay was generated by examining the effect of increasing the starting amount of sample to establish the magnitude of PEG_{mdpnt} score change as a function of assay sample concentration. A randomly selected IgG4P mAb was tested at 4, 2 and 1 mg/mL (Fig. 2). As expected, increasing the sample concentration decreased the PEG_{mdpnt} score. These data suggested that the PEG assay provides a reliable approximation of native state aggregation propensity at high concentrations. Our findings are consistent with other investigators that have demonstrated PEG precipitation-based assays to be a robust indictor of aggregation propensity (Chai *et al.*, 2019; Gibson *et al.*, 2011; Ingham, 1990; Li *et al.*, 2013; Toprani *et al.*, 2016).

Native state aggregation analysis of IgG1 and IgG4 Fc domains

Sequence analysis of IgG1 and IgG4P constant domains revealed substantial charge differences between the Fc domains. To determine the effect of these differences, IgG1 and IgG4P Fc domain constructs (supplementary material, **SI 5**) were produced for analysis in the PEG aggregation assay at pH 7.4 and 5.0. Thermal stability data confirmed that the Fc constructs had T_m values consistent with their respective isotype Fc in the context of an mAb. The IgG1 Fc construct exhibited greater thermal stability than the IgG4 Fc construct at both pH 7.4 and 5.0. Thermal stability of the C_{H2} domains for each isotype was reduced by ~9°C at pH 5.0 (Table II).

At the maximum PEG concentration tested, neither Fc domain reached baseline and therefore PEG_{mdpnt} scores could not be obtained, and instead, aggregation onset scores were used. The IgG1 Fc domain exhibited greater native state aggregation propensity than the IgG4P Fc domain at pH 7.4. Aggregation onset for IgG1 Fc domain was approximately 13.7% PEG 3350, whilst the IgG4P Fc showed no aggregation at 20% PEG 3350 (the highest test PEG 3350 concentration). At pH 5.0, the IgG1 Fc exhibited decreased aggregation propensity. Onset of aggregation occurred at approximately 16.5% PEG. Conversely, the IgG4P Fc exhibited increased native state aggregation propensity at pH 5.0. IgG4P Fc domain aggregation onset occurred at approximately 15% PEG (Fig. 3).

The Fc constructs were analyzed by hydrophobic interaction chromatography (HIC) at pH 7.4 and 5.0. Both constructs had similarly low retention times, suggesting low apparent hydrophobicity. At pH 5.0, both constructs eluted ~3 min earlier compared to pH 7.4, and the IgG4P Fc exhibited a slightly later retention time than the IgG1 Fc construct. It is important to note that at pH 5.0, the IgG1 Fc exhibited decreased thermal stability but showed greater PEG_{mdpnt} score relative to the PEG_{mdpnt} score at pH 7.4 (Table III). It is also noteworthy that the IgG4P Fc showed slightly higher apparent hydrophobicity than the IgG1 Fc but exhibited less apparent native state aggregation propensity.

PEG assay to confirm Fc sequence charge analysis

We examined the impact of intermolecular Fc domain charge interactions by increasing the amount of NaCl in the PEG aggregation assay at pH 5.0. As ionic strength increases, the effective charge on the mAb will decrease due to electrostatic charge shielding, disrupting both attractive and repulsive electrostatic interactions (Curtis *et al.*, 1998). No aggregation was detected at 600 mM of NaCl for both IgG1 and IgG4 Fc constructs (Fig. 4). Thermal stability data showed that increasing the concentration of NaCl slightly decreased thermal stability (Table III). These observations suggested that electrostatic interactions were predominantly responsible for the large difference in aggregation behaviors of the Fc constructs.

Table II. Thermal stability and hydrophobic interaction chromatography (HIC) retention time data for IgG1 Fc and IgG4P Fc constructs in PBS pH 7.4 and 50 mM sodium acetate pH 5.0 125 mM NaCl

Isotype	pH	Thermal stability (°C)	HIC retention time (min)
IgG1	pH 7.4	68.4 ± 0.2	6.2
	pH 5.0	59.3 ± 0.1	2.8
IgG4P	pH 7.4	64.1 ± 0.3	9.0
	pH 5.0	54.9 ± 0.2	6.3

Table III. Thermal stability data for IgG1 Fc and IgG4P Fc in 50 mM of sodium acetate pH 5.0 with 150 mM NaCl, 300 mM NaCl or 600 mM NaCl

		Thermal stability (°C)		
Isotype	pH	150 mM NaCl	300 mM NaCl	600 mM NaCl
IgG1	pH 7.4	68.2 ± 0.2	67.6 ± 0.1	67.2 ± 0.1
	pH 5.0	59.3 ± 0.3	58.3 ± 0.2	57.8 ± 0.1
IgG4P	pH 7.4	64.6 ± 0.1	63.3 ± 0.3	62.7 ± 0.2
	pH 5.0	53.1 ± 0.3	51.9 ± 0.2	50.9 ± 0.3

Table IV. Summary of framework (FW) residue substitutions introduced to $mAbX_{IgG4P}$ and $mAbY_{IgG4P}$

ID	Location	Substitution	HC	LC
M3	FW	Neutral to negative	S70E	S12E, S56E, S67E
M4	FW	Positive to negative	K64E, K75E	R18E, K42E
M5	FW	Positive to neutral	K64Q, K75S	R18S, K42Q

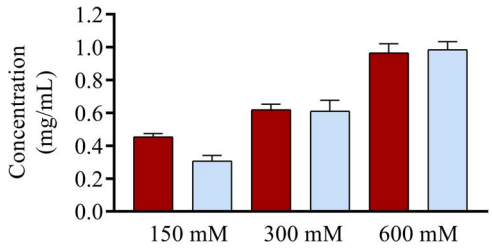

Fig. 4 Bar chart shows concentration of Fc constructs in solution post-24-h incubation at 20°C in 50 mM sodium acetate pH 5.0 20% PEG 3350 with increasing concentrations of sodium chloride. Dark red bars represent IgG1 Fc and light blue bars represent IgG4P Fc. The error bars represent standard deviation from three independent experiments.

Native state aggregation analysis of isotype pairs.

In order to assess the effect of isotype subclass on mAb native state aggregation, we examined seven human IgG1 and IgG4P isotype pairs. Each pair had a unique Fv domain (mAb18, mAb17, mAb19, mAb20, mAb21, mAb10 and mAb13). Thermofluor analysis of the isotype pair mAb panel (supplementary material, **SI 6**) confirmed that the samples had typical thermal stabilities. IgG1 mAbs gave a Fab T_m average of 74.9 ± 4.2°C. As expected, the IgG4P mAb Fab domains exhibited slightly lower thermal stability, with an average T_m value of 71.8 ± 2.7°C (Heads *et al*., 2012; Peters *et al*., 2012).

The sample panel showed a large range of PEG_{mdpnt} scores, and the isotype pairs exhibited markedly different PEG_{mdpnt} scores compared to their counterpart isotype at pH 7.4 and/or 5.0 (Fig. 5A and B, supplementary material, **SI 7–10**). At pH 7.4, five of the seven mAbs showed greater PEG_{mdpnt} scores as an IgG4P isotype. These five Fv domains had net negative charge. The only Fv domain with positive net charge in this set was mAb13 (Fig. 5C and D) which exhibited a greater PEG_{mdnt} score as an IgG1 mAb. mAb17 exhibited a similar PEG_{mdpnt} score as either isotype at pH 7.4 (Fig. 5A). We observed that the IgG1 mAb panel tended to show greater PEG_{mdpnt} scores with decreasing Fv domain net negative charge.

PEG_{mdpnt} scores measured at pH 5.0 revealed further aggregation differences between the mAb isotype pairs. All the IgG1 samples showed a range of improved PEG_{mdpnt} scores at pH 5.0 (Fig. 5B). The magnitude of improvement was greater for samples with less net negative charge. Notably, the IgG1 sample that had a positively charged Fv domain exhibited the greatest improvement. In contrast, the IgG4P samples exhibited similar or worse PEG_{mdpnt} scores at pH 5.0 and did not show the magnitude of improvement to PEG_{mdnt} score observed for many of the IgG1 samples at pH 5.0 (Fig. 5C and D).

Contribution of electrostatic force to mAb aggregation

The difference in PEG_{mdpnt} scores for isotype pairs at pH 7.4 and 5.0 suggested that electrostatic forces initiated mAb native state aggregation. In order to verify the contribution of electrostatic interactions, we examined the effect of increasing ionic strength concentration in the PEG aggregation assay.

Two isotype pairs were selected, one pair sharing a positively charged Fv domain (mAb13 + 4), which exhibited a substantially improved PEG_{mdpnt} score as an IgG1 mAb. and the other isotype pair sharing a negatively charged Fv domain (mAb10 -1), with an improved PEG_{mdpnt} score as the IgG4 isotype. The four samples were buffer exchanged into 10 mM of phosphate pH 7.4 with either 37.5, 150 or 600 mM of NaCl and tested in the PEG

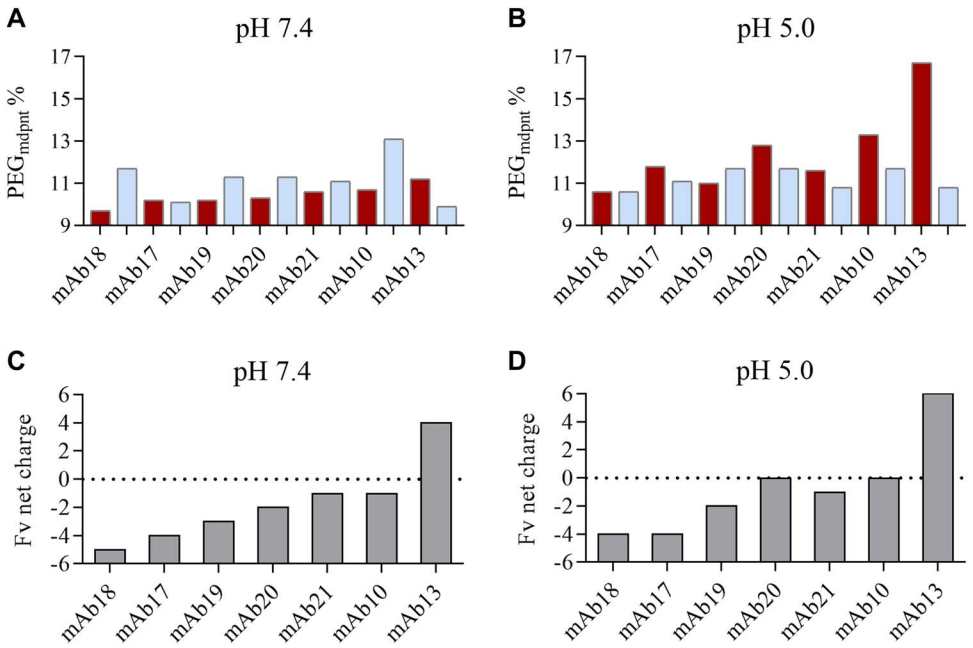

Fig. 5 (**A**) PEG_{mdpnt} data at pH 7.4 for seven variable regions formatted as IgG1 (dark red bars) and IgG4P (light blue bars) isotypes. (**B**) PEG_{mdpnt} data at pH 5.0 for seven variable regions formatted as IgG1and IgG4P isotypes. (**C**) Calculated Fv domain net charge at pH 7.4. (**D**) Calculated Fv domain net charge at pH 5.0 (insufficient sample for replicates).

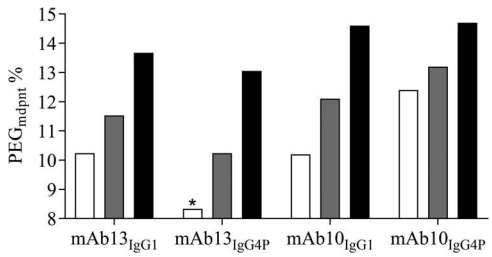

Fig. 6 Bar chart shows PEG_{mdpnt} at pH 7.4 for isotype pair mAbs in various concentrations of NaCl. Hollow bars represent 37.5 mM NaCl, gray bars represent 150 mM NaCl, and black bars represent 600 mM NaCl (insufficient sample for replicates). * sample aggregated at the lowest test concentration of PEG 3350 (7.7%), therefore PEG_{mdpnt} value is an approximation

aggregation assay. At 37.5 mM NaCl, each isotype pair had the largest PEG_{mdpnt} delta, as would be expected due to a low salt shielding effect. At 600 mM NaCl, the difference in PEG_{mdpnt} scores between the two isotypes for each pair was greatly reduced. These data strongly suggested that the difference in PEG_{mdpnt} scores between the IgG1 and IgG4P isotypes is a result of intermolecular electrostatic interactions (Fig. 6, supplementary material, **SI 11–14**).

Fv domain charge substitutions

The following framework (FW) amino acid residue substitution strategy was designed to test our electrostatic inter-domain aggregation hypothesis. Note that these predictions are based on an IgG4P mAb with a positively charged Fv domain at pH 7.4.

1. Neutral to negative substitutions—predicted to show reduced aggregation at pH 7.4 but greater aggregation at pH 5.0
2. Positive to negative substitutions—predicted to show reduced aggregation at pH 7.4 but greater aggregation at pH 5.0
3. Positive to neutral substitutions—predicted to show reduced native state aggregation at pH 7.4 and 5.0

Our isotype pair data suggested that an IgG4P mAb with a positively charged Fv domain at pH 7.4 would have a high aggregation propensity. We therefore selected two IgG4P mAbs with positively charged Fv domains for analysis, $mAbX_{IgG4P}$ and $mAbY_{IgG4P}$ (+5 and + 6 respectively at pH 7.4), each having a unique Fv domain that bind different ligands. These two mAbs were not part of the isotype pair sample set. Residue substitutions were introduced to the FWs, each replacement residue was selected by referring to abYsis, a web-based database of antibody sequence that includes a set of residue frequency tables for each position in an antibody (Martin, 1996; Swindells *et al*., 2017). To minimize the risk of introducing destabilizing FW residue substitutions, only surface-exposed residues where the side-chain was not observed to H-bond to other side chains were selected (Fig. 7 **and** Table IV).

Analysis of charge variants

Thermal stability data indicated that all the samples were folded and comparable to wild type (WT) and that the molecules had thermal stabilities comparable to commercially available mAb therapeutics (Jain *et al*., 2017). Residue substitutions in the FW regions resulted in relatively minor affinity differences compared to WT (Table V).

Native state aggregation analysis of WT and charge variants

The PEG aggregation assay was used to determine native state aggregation propensity of $mAbX_{IgG4P}$ and $mAbY_{IgG4P}$ WT and

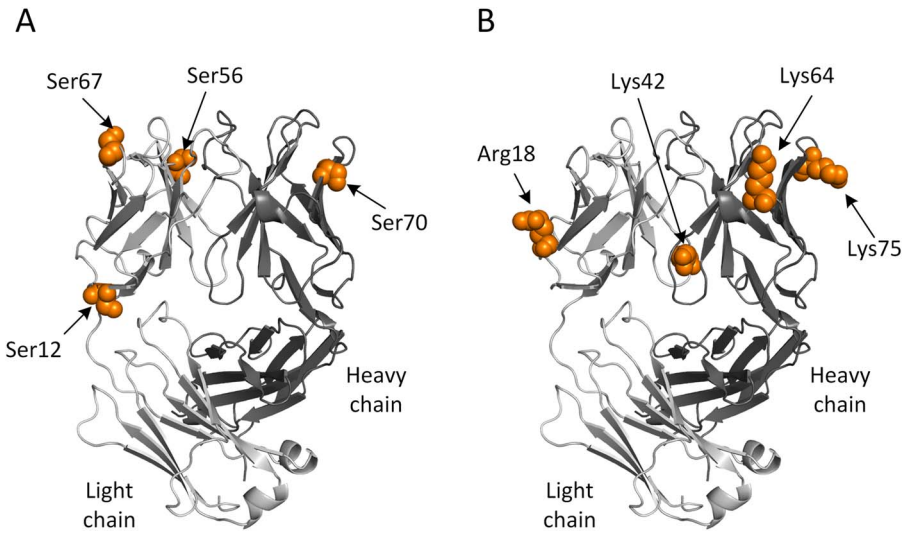

Fig. 7 Sites of residues mutated to alter the charge of the Fv. The residues are solvent-exposed and considered amenable to mutation with minimal or no impact on antibody structure. (**A**) Neutral Ser residues which were substituted with negative Glu and (**B**) positive Arg or Lys residues which were substituted with either negative Glu or neutral Ser or Gln. The residues have been superimposed onto the crystal structure of a humanized Fab fragment (PDB code 5FUZ).

Table V. Summary of pI, thermal stability and Biacore data for $mAbX_{IgG4P}$ and $mAbY_{IgG4P}$ with and without residue substitutions

	Calculated pI		Calculated charge pH 7.4		Calculated charge pH 5.0		Fab domain Tm (°C)		Biacore (KD μM)	
	mAbX	mAbY	mAbX	mAbY	mAbX	mAbY	mAbX	mAbY	mAbX	mAbY
WT	9.0	9.1	5	6	5	9	78.2 ± 0.1	74.2 ± 0.1	7.6	0.71
M3	7.7	8.4	1	2	1	5	77.7 ± 0.1	74.1 ± 0.1	11.3	1.41
M4	6.2	6.5	-3	-2	-3	1	77.6 ± 0.1	72.5 ± 0.1	6.5	1.01
M5	7.7	8.4	1	2	1	5	77.2 ± 0.1	76. 2 ± 0.1	7.4	0.96

charge variants. All the substitutions improved the PEG_{mdpnt} scores at pH 7.4 compared to WT as predicted. FW variant M3 (four neutral to negative residue substitutions) resulted in a comparatively modest improvement to PEG_{mdnt} score for both mAbs. The M4 variant (four positive to negative residue substitutions) had a greater beneficial effect for $mAbX_{IgG4P}$. This was attributed to the greater net positive charge of $mAbY_{IgG4P}$. The introduction of negatively charged residues to the FW increases the relative probability of electrostatic attraction events due to the comparatively high number of positively charged residues of $mAbY_{IgG4P}$. The M5 variant (four positive to neutral residue substitutions) resulted in a substantial increase in PEG_{mdnt} score for both molecules.

A comparison of PEG_{mdnpt} scores for $mAbX_{IgG4P}$ and $mAbY_{IgG4P}$ measured at pH 5.0 revealed significant differences in aggregation scores (Fig. 8A and B, supplementary material, **SI 15–18**). WT PEG_{mdpnt} score was increased for both mAbs as expected at pH 5.0 due to a greater probability of charge repulsion events caused by the greater number of positively charged residues at this slightly acidic pH. M3 showed a similar PEG_{mdpnt} score at pH 5.0 and 7.4 for $mAbX_{IgG4P}$ and a slightly decreased PEG_{mdpnt} score for $mAbY_{IgG4P}$. M4 showed a decrease in PEG_{mdpnt} scores at pH 5.0. The substitution of positively charged residues with negatively charged residues resulted in a greater probability of electrostatic attractions at pH 5.0 as predicted. Again, $mAbY_{IgG4P}$ showed the largest decrease. Substituting positive framework residues with neutral residues (M5) resulted in an increased PEG_{mdpnt} score compared to WT at pH 7.4 for both test mAbs and decreased aggregation propensity at pH 5.0.

Discussion

Therapeutic mAbs are often required to be stable at high concentrations (>100 mg/mL) for subcutaneous (SC) administration (Jin *et al*., 2015); therefore, it is important to select molecules that exhibit low aggregation propensity at these elevated concentrations. In addition, it is preferred that therapeutic mAbs are stable at the various pH values required by manufacturing processes. Aggregation propensity can be mitigated by formulation; however, this process can result in prolonged development times (Razinkov *et al*., 2015). Furthermore, post SC administration, the local concentration of therapeutic mAb remains high (Richter and Jacobsen, 2014), while the ionic strength, buffering capacity and excipients are diminished (Turner and Balu-Iyer, 2018). A shift to the physiological pH value of SC tissue could compromise stability of the mAb and lead to the formation of aggregates (Kinnunen and Mrsny, 2014), which have been associated with immune responses to drug and poor bioavailability (Dobson *et al*., 2016; Vugmeyster *et al*., 2012). The aim of this work was to develop a sequence-based methodology that facilitates the selection, design and production of IgG1 and IgG4P mAbs with reduced aggregation propensity at acidic and neutral pH.

Few published studies have examined the impact of antibody isotype on aggregation propensity. Those that have were limited in

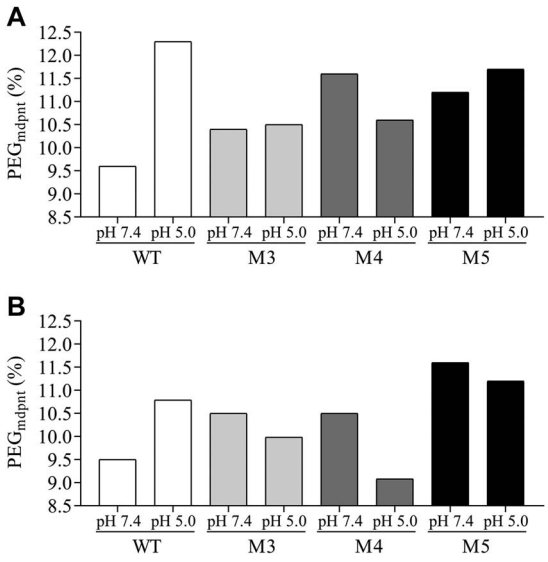

Fig. 8 (**A**) Bar chart showing PEG_{mdpnt} score for $mAbX_{IgG4P}$ WT and FW substitutions. The first and second bar within each group shows samples analyzed at pH 7.4 and 5.0, respectively. (**B**) Bar chart showing PEG_{mdpnt} score for $mAbY_{IgG4P}$ WT and FW substitutions (insufficient sample for replicates).

scope, typically examining a single parent Fv domain. Pepinsky et al. (Pepinsky *et al*., 2010) showed that switching isotype subclass greatly reduced the aggregation propensity of an IgG1 mAb with remarkably poor solubility (visible aggregate at < 1 mg/mL). Bethea et al. reported that CNTO607, an IgG1 mAb generated by phage display, aggregated at ~ 13 mg/mL in PBS, and after an isotype switch to the IgG4P subclass no visible aggregate was detected at 110 mg/mL (Bethea *et al*., 2012). Neergard et al. (Neergaard *et al*., 2014) used a broad range of analytical techniques to compare the stability differences of an IgG1 mAb and an IgG4P mAb with the same Fv domain at > 150 mg/mL. The IgG4P mAb exhibited greater aggregation at pH 5.0 and 7.4 both isotypes showed relatively low aggregation propensity. These case studies were not designed to establish the cause of isotype-dependent native state aggregation propensity.

IgG1 and IgG4 constant domains share $\sim 95\%$ sequence homology; sequence analysis performed by Chennamsetty et al.,(Chennamsetty *et al*., 2009) suggested that the constant domains of each isotype share similar hydrophobic profiles. Our experimental data indicated that both Fc domains exhibit low hydrophobicity consistent with their prediction. The most prominent sequence difference between the constant domains is the number of positively and negatively charged amino acids. The IgG4P Fc has calculated pI of 6.0, while the calculated pI of the IgG1 Fc is 7.8.

Analysis of Fc domains in the PEG aggregation assay indicated that the IgG1 Fc domain had greater native state aggregation propensity than the IgG4P Fc domain at pH 7.4. To examine the effect of charge states, IgG1 and IgG4P Fc domains were tested at pH 5.0. Due to protonation of histidine residues at this slightly acidic pH, both Fc domains have increased net positive charge. At pH 5.0, native state aggregation propensity is decreased for the IgG1 Fc domain and increased for the IgG4 Fc domain. Thermal stability and hydrophobic interaction chromatography data suggested that conformational stability and hydrophobicity differences were unlikely to be responsible for the different native aggregation propensities of IgG1 and IgG4 Fc domains at pH 7.4 and 5.0. Therefore, the change in relative aggregation propensity for each Fc domain is likely due to electrostatic interactions rather than conformational or hydrophobic differences.

The increased probability of electrostatic repulsion/decreased probability of electrostatic attraction could explain the lower aggregation propensity of the negatively charged IgG4P Fc compared to the IgG1 Fc at pH 7.4. At pH 5.0, both samples gain positive charge and, as expected, the IgG1 Fc exhibited reduced aggregation, most likely caused by greater electrostatic repulsion. The increased aggregation propensity observed for the IgG4 Fc construct at pH 5.0 could be attributed to the relatively high number of negatively charged residues. The increased availability of positively charged residues at pH 5.0 would increase the probability of attractive electrostatic interactions, thereby promoting aggregation events.

To confirm the contribution of electrostatic interactions, each Fc domain was analyzed in the PEG aggregation assay with increasing amounts of NaCl. As the ionic strength was increased, attractive and repulsive electrostatic interactions were diminished. The difference between PEG_{mdpnt} scores for the Fc subclasses was reduced at high ionic strength. This result indicated that electrostatic interactions were predominately responsible for the different native state aggregation propensities of the IgG1 and IgG4P Fc domains.

Based on our Fc domain observations, we hypothesized that at pH 7.4, a Fv domain with net negative charge would permit a greater frequency of attractive electrostatic interactions as an IgG1 mAb. The same Fv domain formatted as an IgG4P mAb would have a lower frequency of attractive electrostatic interactions, and a greater probability of repulsive interactions, decreasing the probability of native aggregation compared to the IgG1 isotype. Conversely, at pH 5.0 (greatly increasing the number of positively charged residues), a Fv domain with net negative charge would permit an increased frequency of attractive electrostatic interactions as an IgG4 mAb due to the greater number of acidic residues in this isotype. Following this logic, an Fv domain with net positive charge would have a greater propensity for native state aggregation as an IgG4P mAb at pH 7.4 and 5.0 compared to the IgG1 mAb (Fig. 9).

To substantiate our hypothesis, we produced seven human IgG1 and IgG4P isotype pairs each having a unique Fv domain that binds different ligands. We found that IgG1 mAbs with negatively charged Fv domains showed equal or lower PEG_{mdpnt} scores compared to the counterpart IgG4P mAb at pH 7.4.

At pH 5.0, the IgG1 mAb panel exhibited greater PEG_{mdnt} scores relative to the pH 7.4 result. Notably, the magnitude of improvement was greater for IgG1 samples that had Fv domains with no net charge or positive net charge. Consistent with our hypothesis, IgG4P mAbs with net negatively charged Fv domains showed similar or lower PEG_{mdpnt} scores at pH 5.0 relative to the pH 7.4 scores. We reasoned that the higher PEG_{mdnt} score at pH 5.0 for IgG1 mAbs is most likely due to the IgG1 Fc having fewer negatively charged residues reducing the frequency of unfavourable electrostatic interactions compared to the counterpart IgG4P mAb.

To confirm that electrostatic interactions were responsible for the different aggregation behaviors, salt shielding experiments were performed. Two isotype pairs were selected from our sample set, each pair having either a positively charged or negatively charged Fv domain. The positively charged Fv domain exhibited a greater PEG_{mdnt} score as the IgG1 isotype, and the negatively charged Fv domain showed a greater PEG_{mdnt} score as the IgG4 isotype. Addition of high concentrations of NaCl to disrupt electrostatic

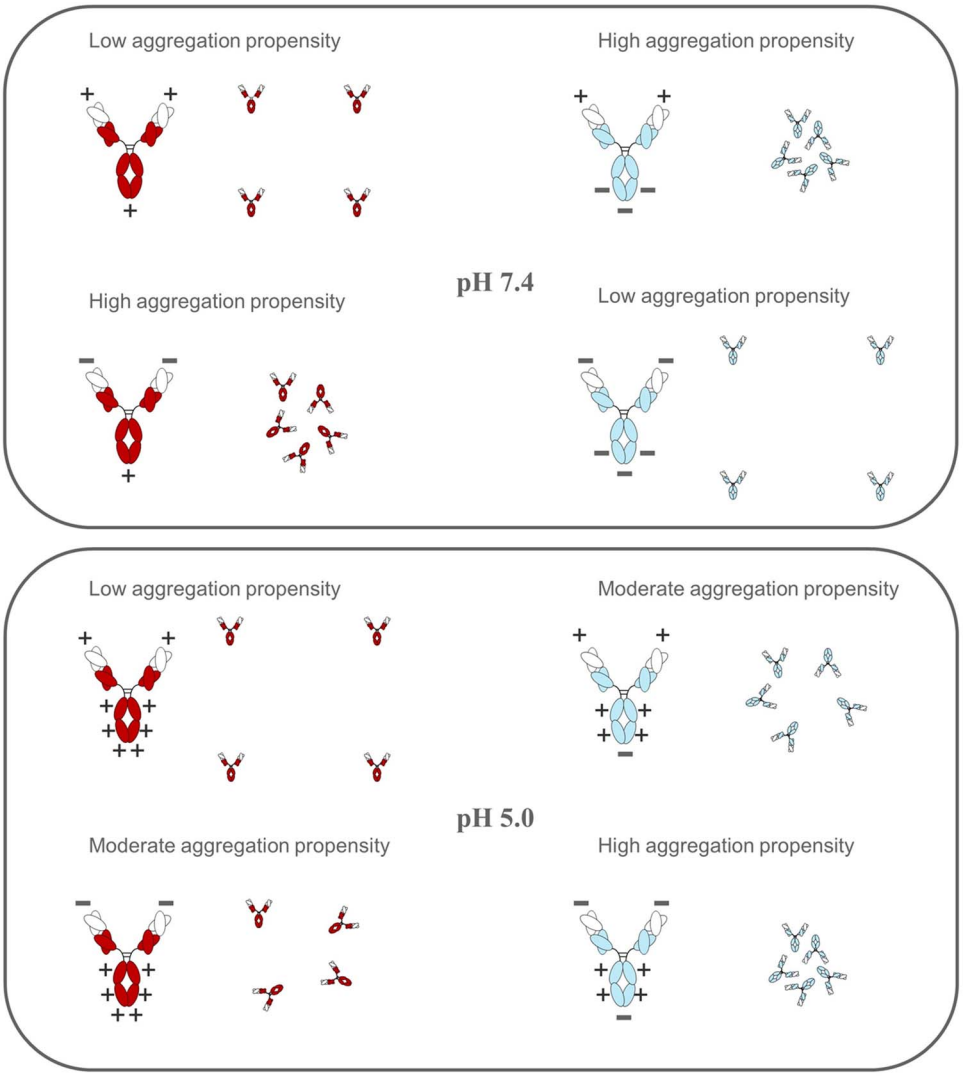

Fig. 9 Illustration shows simplified differential electrostatic aggregation model for IgG1 (dark red) and IgG4P (light blue) mAbs with positive or negative charged Fv domains at pH 7.4 and 5.0. Shorter distance between molecules represents greater probability of charge attraction events (greater probability of native state aggregation). Charge signs are a visual guide and do not depict actual net charge of domains.

interactions resulted in similar PEG_{mdpnt} scores for each isotype pair. These results indicated that intermolecular electrostatic interactions were predominately responsible for the different aggregation propensities of the isotype pairs.

Having demonstrated a charge-based mechanism of isotype-dependent mAb native state aggregation (for isotype pairs with the same Fv and thus similar overall hydrophobicity), we next designed a series of rational residue substitutions to determine the optimal strategy for decreased aggregation propensity at pH 7.4 and 5.0. We selected two IgG4P mAbs, $mAbX_{IgG4P}$ and $mAbY_{IgG4P}$, each with unique Fv domains that bind different ligands for analysis. These mAbs were not part of the isotype pair mAb test panel, nor had they contributed to the generation of the hypothesis. Both had Fv domains with high pI values and exhibited low PEG_{mdpnt} scores (<10). At pH 7.4, the Fv domains of these IgG4P mAbs have significant net positive charge (+5 and + 6 respectively); therefore, based on our IgG4P mAb aggregation model, a reduction in net positive charge was predicted to reduce aggregation propensity. To minimize the risk of introducing destabilizing framework residue substitutions, only surface-exposed residues where the side-chain was not observed to H-bond to other side chains were selected. The abYsis database was used to select framework residues for substitution based on human germline sequence. At each selected position naturally occurring human residues were used to replace the target residue (Swindells *et al*., 2017), thus minimizing immunogenicity risk.

There are several residue substitution strategies that lower net charge, each with a predictable outcome based on our electrostatic aggregation model. Positive to neutral substitutions: predicted to show reduced native state aggregation at pH 7.4 and 5.0. Positive to negative substitutions: predicted to show reduced aggregation at pH 7.4 but greater aggregation at pH 5.0. Neutral to negative substitutions: predicted to show reduced aggregation at pH 7.4 but greater aggregation at pH 5.0.

All the substitutions improved the PEG_{mdpnt} scores at pH 7.4 compared to the WT mAbs as predicted. The removal of positively charged residues rather than the introduction of negatively charged residues tended to show greater PEG_{mdpnt} improvement. The aggregation behavior at pH 5.0 for each variant was also consistent

with our charge-based native state aggregation model. At slightly acidic pH, there was a substantial increase in positive charge largely due to the protonation of histidine residues. This resulted in an improved PEG_{mdpnt} score for each WT sample as expected due to a greater probability of electrostatic repulsion events. The difference in magnitude of improvement at pH 5.0 for the two WT samples could be attributed to the number of histidine residues in the Fv domain. Sequence analysis revealed that $mAbY_{IgGF4P}$ had three histidine residues in the Fv domain and $mAbX_{IgG4P}$ had none. It is plausible that these residues increase the probability of unfavourable intermolecular electrostatic interactions for $mAbY_{IgG4P}$.

Substitution of neutral framework residues with negatively charged residues (M3—S70E, S12E, S56E, S67E) resulted in a similar or slightly lower PEG_{mdnt} at pH 5.0 compared to the pH 7.4 result. This is explained by a greater probability of charge attraction events due to the increased number of negatively charged residues in the framework. The greater number of positively charged residues of $mAbY_{IgG4P}$ would increase the frequency of electrostatic interactions which could explain the decreased PEG_{mdpnt} score relative to the pH 7.4 score. Substituting positively charged residues with negatively charged residues (M4—K64E, K75E, R18E, K42E) resulted in markedly lower PEG_{mdpnt} scores at pH 5.0. This outcome was expected, as these residue substitutions simultaneously increase the probability of electrostatic attraction events whilst decreasing the probability of repulsion events. Substituting positive framework residues with neutral residues (M5—K64Q, K75S, R18S, K42Q) resulted in greatly increased PEG_{mdnt} scores at both pH 7.4 and 5.0 for each sample compared to their respective WT at pH 7.4. Counter to the improvement at pH 5.0 observed for $mAbX_{IgG4P}$ M5, there was a slight decrease in PEG_{mdpnt} score for $mAbY_{IgG4P}$ M5 relative to the pH 7.4 M5 PEG_{mdpnt} score. This is probably due to the three histidine residues in the framework region of $mAbY_{IgG4P}$ resulting in a greater likelihood of electrostatic attractions. We applied our residue substitution strategy to several positively charged residues in the complementarity-determining region of $mAbX_{IgG4P}$ and $mAbY_{IgG4P}$ (supplementary material, **SI 19–24**). The observed aggregation behaviors were consistent with the framework charge variants. However, as might be expected, the residue substitutions ablated affinity. Nevertheless, this would be a viable strategy for mAbs with known paratopes or for curated affinity maturation.

It is often stated that proteins with pI values away from the buffer pH will have a decreased risk of aggregation due to repulsive electrostatic interactions (Laue, 2012; van der *et al*., 2017; Wu *et al*., 2010). Our data contradict this simplistic model. Both WT IgG4P test mAbs have high pI values ($\geq$ 9.0), and at pH 7.4, each sample exhibited relatively low PEG_{mdpnt} scores, indicating high native state aggregation propensity. The rationally designed residue substitutions reduced the pI and decreased native state aggregation for all the test molecules at pH 7.4. This apparent contradiction is explained by the method(s) used to determine pI (which do not consider ionic strength) and the increased probability of charge distribution effects for large multidomain proteins such as mAbs.

Our data strongly suggest that aggregation propensity can be predicted by analysis of Fv domain net charge sign in relation to isotype subclass, and that reduction of Fv domain net charge is an effective method to decrease mAb native state aggregation propensity. Reduced net charge is most efficiently achieved by substituting a charged residue by a residue of opposite charge. Importantly, we have demonstrated that this is not an optimal strategy for generating therapeutic molecules. Such mutations can increase the risk of aggregation when samples are exposed to shifts in pH. It is therefore best to substitute charged residues that drive the undesirable electrostatic interactions, with neutral polar residues, thereby avoiding the potential for attractive electrostatic interactions at altered pH states.

Other investigators have explored mAb intermolecular domain interactions; however, these studies are predominately based on the viscosity of IgG1 mAbs at $>$ 100 mg/mL and not native state aggregation. These reports have been based on a single mAb or from coarse grained computational models of IgG1 mAbs (Chaudhri *et al*., 2012; Arora *et al*., 2016). To the best of our knowledge, this is the first experimentally substantiated description of isotype-dependent native state aggregation mediated by Fv domain– constant domain interaction.

Native state aggregation propensity is driven by numerous variables such as charge, hydrophobicity and conformational flexibility. Our aim was not to predict absolute native aggregation propensity, but rather to elucidate the cause for differential aggregation of IgG1 and IgG4P mAbs with the same Fv domain. Specific charge variants informed by our differential electrostatic aggregation model suggests a new approach for increasing mAb developability. We expect the results presented here to be of use in generating improved *in silico* aggregation prediction tools that tend to simplify electrostatic effects (Lauer *et al*., 2012; Wolf Perez *et al*., 2018).

In conclusion, the different aggregation propensity of an Fv domain formatted as either IgG1 or IgG4P isotype can be predicted from the linear amino acid sequence. This finding enables the selection or rational design of therapeutic mAb candidates with reduced aggregation potential. In addition, optimal buffer pH can be predicted for improved long-term storage and streamlined formulation studies, decreasing the development cost and time to market of therapeutic mAbs.

Supplementary data

Supplementary data are available at PEDS online.

Acknowledgments

We would like to thank Andy Popplewell, David Humphreys, Sam Heywood and Shirley Peters for their support, helpful discussions and critical review of this work.

Author Contributions

All authors contributed equally to the generation of this manuscript.

Conflict of Interest

No potential conflict of interests.

References

Angal, S., King, D.J., Bodmer, M.W. *et al.* (1993) A single amino acid substitution abolishes the heterogeneity of chimeric mouse/human (IgG4) antibody. *Mol. Immunol.*, **30**, 105–108.

Arora, J., Hu, Y., Esfandiary, R. *et al.* (2016) Charge-mediated fab-fc interactions in an IgG1 antibody induce reversible self-association, cluster formation, and elevated viscosity. *MAbs*, **8**, 1561–1574.

Atha, D.H. and Ingham, K.C. (1981) Mechanism of precipitation of proteins by polyethylene glycols. Analysis in terms of excluded volume. *J. Biol. Chem.*, **256**, 12108–12117.

Baert, F., Noman, M., Vermeire, S. et al. (2003) Influence of immunogenicity on the long-term efficacy of infliximab in Crohn's disease. *N. Engl. J. Med.*, **348**, 601–608.

Bergmann-Leitner, E.S., Mease, R.M., Duncan, E.H., Khan, F., Waitumbi, J., Angov, E. (2008) Evaluation of immunoglobulin purification methods and their impact on quality and yield of antigen-specific antibodies. *Malar. J.*, **7**, 129.

Bethea, D., Wu, S.J., Luo, J. *et al.* (2012) Mechanisms of self-association of a human monoclonal antibody CNTO607. *Protein Eng. Des. Sel.*, **25**, 531–537.

Chai, Q., Shih, J., Weldon, C., Phan, S., Jones, B.E. (2019) Development of a high-throughput solubility screening assay for use in antibody discovery. *MAbs*, **11**, 747–756.

Chaudhri, A., Zarraga, I.E., Kamerzell, T.J. *et al.* (2012) Coarse-grained modeling of the self-association of therapeutic monoclonal antibodies. *J. Phys. Chem. B*, **116**, 8045–8057.

Chennamsetty, N., Helk, B., Voynov, V., Kayser, V., Trout, B.L. (2009) Aggregation-prone motifs in human immunoglobulin G. *J. Mol. Biol.*, **391**, 404–413.

Cromwell, M.E., Hilario, E., Jacobson, F. (2006) Protein aggregation and bioprocessing. *AAPS J.*, **8**, E572–E579.

Curtis, R.A., Montaser, A., Prausnitz, J.M., Blanch, H.W. (1998) Protein-protein and protein-salt interactions in aqueous protein solutions containing concentrated electrolytes. *Biotechnol. Bioeng.*, **58**, 451.

Dobson, C.L., Devine, P.W., Phillips, J.J. *et al.* (2016) Engineering the surface properties of a human monoclonal antibody prevents self-association and rapid clearance in vivo. *Sci. Rep.*, **6**, **38644**.

Gibson, T.J., Mccarty, K., Mcfadyen, I.J. *et al.* (2011) Application of a high-throughput screening procedure with PEG-induced precipitation to compare relative protein solubility during formulation development with IgG1 monoclonal antibodies. *J. Pharm. Sci.*, **100**, 1009–1021.

Heads, J.T., Adams, R., D'Hooghe, L.E. *et al.* (2012) Relative stabilities of IgG1 and IgG4 fab domains: Influence of the light-heavy interchain disulfide bond architecture. *Protein Sci.*, **21**, 1315–1322.

Ingham, K.C. (1990) Precipitation of proteins with polyethylene glycol. *Methods Enzymol.*, **182**, 301–306.

Jain, T., Sun, T., Durand, S. *et al.* (2017) Biophysical properties of the clinical-stage antibody landscape. *Proc. Natl. Acad. Sci. U. S. A.*, **114**, 944–949.

Jarasch, A., Koll, H., Regula, J.T., Bader, M., Papadimitriou, A., Kettenberger, H. (2015) Developability assessment during the selection of novel therapeutic antibodies. *J. Pharm. Sci.*, **104**, 1885–1898.

Jin, J.F., Zhu, L.L., Chen, M. *et al.* (2015) The optimal choice of medication administration route regarding intravenous, intramuscular, and subcutaneous injection. *Patient Prefer. Adherence*, **9**, 923–942.

Kinnunen, H.M. and Mrsny, R.J. (2014) Improving the outcomes of biopharmaceutical delivery via the subcutaneous route by understanding the chemical, physical and physiological properties of the subcutaneous injection site. *J. Controlled Release: Off. J. Controlled Release Soc.*, **182**, 22–32.

Knevelman, C., Davies, J., Allen, L., Titchener-Hooker, N.J. (2010) High-throughput screening techniques for rapid PEG-based precipitation of IgG4 mAb from clarified cell culture supernatant. *Biotechnol. Prog.*, **26**, 697–705.

Kola, I. and Landis, J. (2004) Can the pharmaceutical industry reduce attrition rates? *Nat. Rev. Drug Discov.*, **3**, 711–715.

Laue, T. (2012) Proximity energies: A framework for understanding concentrated solutions. *J. Mol. Recognit.*, **25**, 165–173.

Lauer, T.M., Agrawal, N.J., Chennamsetty, N., Egodage, K., Helk, B., Trout, B.L. (2012) Developability index: A rapid in silico tool for the screening of antibody aggregation propensity. *J. Pharm. Sci.*, **101**, 102–115.

Lehninger, A., Cox, M.M., Nelson, D.L. (2008) *Lehninger Principles of Biochemistry and Absolute Ultimate Guide*. W.H. Freeman and Company: New York.

Li, L., Kantor, A., Warne, N. (2013) Application of a PEG precipitation method for solubility screening: A tool for developing high protein concentration formulations. *Protein sci.: A publication of the Protein Soc.*, **22**, 1118–1123.

Liu, H.F., Ma, J., Winter, C., Bayer, R. (2010) Recovery and purification process development for monoclonal antibody production. *MAbs*, **2**, 480–499.

Martin, A.C. (1996) Accessing the Kabat antibody sequence database by computer. *Proteins*, **25**, 130–133.

Martinez, M., Spitali, M., Norrant, E.L., Bracewell, D.G. (2019) Precipitation as an enabling technology for the intensification of biopharmaceutical manufacture. *Trends Biotechnol.*, **37**, 237–241.

Moussa, E.M., Panchal, J.P., Moorthy, B.S. *et al.* (2016) Immunogenicity of therapeutic protein aggregates. *J. Pharm. Sci.*, **105**, 417–430.

Neergaard, M.S., Nielsen, A.D., Parshad, H., Van De Weert, M. (2014) Stability of monoclonal antibodies at high-concentration: Head-to-head comparison of the IgG1 and IgG4 subclass. *J. Pharm. Sci.*, **103**, 115–127.

Pepinsky, R.B., Silvian, L., Berkowitz, S.A. *et al.* (2010) Improving the solubility of anti-LINGO-1 monoclonal antibody Li33 by isotype switching and targeted mutagenesis. *Protein Sci.: A Publication of the Protein Soc.*, **19**, 954–966.

Peters, S.J., Smales, C.M., Henry, A.J., Stephens, P.E., West, S., Humphreys, D.P. (2012) Engineering an improved IgG4 molecule with reduced disulfide bond heterogeneity and increased fab domain thermal stability. *J. Biol. Chem.*, **287**, 24525–24533.

Pineda, C., Castaneda Hernandez, G., Jacobs, I.A., Alvarez, D.F., Carini, C. (2016) Assessing the immunogenicity of biopharmaceuticals. *BioDrugs: Clinical Immunotherapeutics, Biopharmaceuticals and Gene Therapy*, **30**, 195–206.

Polson, A., Potgieter, G.M., Largier, J.F., Mears, G.E., Joubert, F.J. (1964) The fractionation of protein mixtures by linear polymers of high molecular weight. *Biochim. Biophys. Acta*, **82**, 463–475.

Razinkov, V.I., Treuheit, M.J., Becker, G.W. (2015) Accelerated formulation development of monoclonal antibodies (mAbs) and mAb-based modalities: Review of methods and tools. *J. Biomol. Screen.*, **20**, 468–483.

Richter, W.F. and Jacobsen, B. (2014) Subcutaneous absorption of biotherapeutics: Knowns and unknowns. *Drug Metab. Dispos.*, **42**, 1881–1889.

Roopenian, D.C. and Akilesh, S. (2007) FcRn: The neonatal fc receptor comes of age. *Nat. Rev. Immunol.*, **7**, 715–725.

Shire, S.J. (2009) Formulation and manufacturability of biologics. *Curr. Opin. Biotechnol.*, **20**, 708–714.

Shire, S.J., Shahrokh, Z., Liu, J. (2004) Challenges in the development of high protein concentration formulations. *J. Pharm. Sci.*, **93**, 1390–1402.

Singh, S.K. (2011) Impact of product-related factors on immunogenicity of biotherapeutics. *J. Pharm. Sci.*, **100**, 354–387.

Swindells, M.B., Porter, C.T., Couch, M. *et al.* (2017) abYsis: Integrated antibody sequence and structure-management, analysis, and prediction. *J. Mol. Biol.*, **429**, 356–364.

Toprani, V.M., Joshi, S.B., Kueltzo, L.A., Schwartz, R.M., Middaugh, C.R., Volkin, D.B.A. (2016) Micro-polyethylene glycol precipitation assay as a relative solubility screening tool for monoclonal antibody design and formulation development. *J. Pharm. Sci.*, **105**, 2319–2327.

Turner, M.R. and Balu-Iyer, S.V. (2018) Challenges and opportunities for the subcutaneous delivery of therapeutic proteins. *J. Pharm. Sci.*, **107**, 1247–1260.

Vidarsson, G., Dekkers, G., Rispens, T. (2014) IgG subclasses and allotypes: From structure to effector functions. *Front. Immunol.*, **5**, 520.

Vugmeyster, Y., Xu, X., Theil, F.P., Khawli, L.A., Leach, M.W. (2012) Pharmacokinetics and toxicology of therapeutic proteins: Advances and challenges. *World J. Biol. Chem.*, **3**, 73–92.

Wang, W. and Roberts, C.J. (2018) Protein aggregation - mechanisms, detection, and control. *Int. J. Pharm.*, **550**, 251–268.

Wang, W., Singh, S., Zeng, D.L., King, K., Nema, S. (2007) Antibody structure, instability, and formulation. *J. Pharm. Sci.*, **96**, 1–26.

Wolf Perez, A.M., Sormanni, P., Andersen, J.S.,Sakhnini, LI, Rodriguez-Leon, I, Bjelke, JR, *et al.* (2019). In vitro and in silico assessment of the developability of a designed monoclonal antibody library. *mAbs.* **11**, 388–400.

Wu, S.J., Luo, J., O'Neil, K.T. *et al.* (2010) Structure-based engineering of a monoclonal antibody for improved solubility. *Protein Eng. Des. Sel.*, **23**, 643–651.

van der, R., Karow-Zwick, A.R., Van Durme, J. *et al.* (2017) Prediction and reduction of the aggregation of monoclonal antibodies. *J. Mol. Biol.*, **429**, 1244–1261.